J. Phys. A: Math. Gen. **31** (1998) 7141–7155. Printed in the UK PII: S0305-4470(98)85411-5

Nonlinear Galerkin methods based on the concept of determining modes for the magnetohydrodynamic equations

Olaf Schmidtmann†§, Fred Feudel‡ and Norbert Seehafer‡

† Weierstraß-Institut für Angewandte Analysis und Stochastik, Mohrenstraße 39, D-10117 Berlin, Germany

‡ Universität Potsdam, Institut für Theoretische Physik and Astrophysik, PF 601553, D-14415 Potsdam, Germany

Received 27 June 1997, in final form 13 February 1998

Abstract. A new nonlinear Galerkin method based on an approximate inertial manifold and on a finite number of determining modes has been implemented for the three-dimensional magnetohydrodynamic equations. It is found that these active modes, which regulate the dynamics of the system, are not necessarily those with the smallest wavenumbers but those containing most of the time-averaged enstrophy. It is demonstrated that owing to the reduced number of equations the modified nonlinear Galerkin method, which includes only these determining modes in a truncation, improves the computational efficiency in comparison with the traditional Galerkin method.

1. Introduction

For numerical investigations of certain nonlinear dissipative partial differential equations (PDEs) it is necessary to approximate the solutions to the *a priori* infinite-dimensional problem by solutions to a finite-dimensional system of ordinary differential equations (ODEs). One usually expands the solution into a Fourier series, constructs a system of infinitely many ODEs for the Fourier coefficients and truncates the system dropping the smaller wavenumbers. This procedure, known as the linear or traditional Galerkin method, provides a finite-dimensional approximation for the Fourier modes.

The qualitative behaviour of solutions to this finite-dimensional system, however, strongly depends on the number of modes taken into account. An approximation with too few modes may lead to solutions whose long-term behaviour is completely different from those in the original system. Thus, the number of necessary equations (dimension of the phase space) may be very large, as for example, in hydrodynamics and magnetohydrodynamics (MHD) for the case of high Reynolds numbers, and the numerical computation of these high-dimensional problems is nearly impossible with capacities of currently available computers.

A very important property of dissipative differential equations is that after a transient period of time the state of the system converges to an attractor whose dimension is less than the dimension of the phase space (Swinney and Gollub 1985, Manneville 1990). Therefore one is inspired to reduce the dimension of the problem by splitting the solution in master

§ E-mail address: schmidtmann@wias-berlin.de

0305-4470/98/347141+15$19.50

modes, essentially determining the dynamics of the system, and in so-called slaved modes as a function of them.

The theory of inertial manifolds (IM) and approximate inertial manifolds (AIM) was introduced 10 years ago by Temam (1988) to provide such a function. In connection with this theory nonlinear Galerkin methods have been developed by Temam and Marion (1989) to study the long-term behaviour of certain dissipative PDEs. The essential aim of these methods is to characterize high-dimensional nonlinear differential equations by low-dimensional equations without losing the qualitative properties of the original system. Many publications suggest that these approximations, based on nonlinear Galerkin techniques, are more efficient than traditional Galerkin methods (Dubois *et al* 1991, Foias *et al* 1988, Jauberteau *et al* 1989/90, Frisch *et al* 1986, Foias *et al* 1988a).

An IM is a finite-dimensional positively invariant Lipschitz-manifold which attracts all trajectories at an exponential rate. It contains the global attractor, whenever it exists (cf Temam 1988, 1989, 1990, Foias *et al* 1988, 1989). In the limit of infinite time the solutions to the PDE lie on the IM; the PDE is reduced to a finite system of ODEs. For several PDEs such as the Kuramoto–Sivashinsky, Cahn–Hillard and Ginzburg–Landau equations there exists an IM (Foias *et al* 1988c, 1988, Temam 1988). The existence of an IM for both the Navier–Stokes equations (NSE) and the MHD equations is still an open problem.

Therefore the concept of AIM has been introduced by Foias *et al* (1988b) for two-dimensional (2D) NSE. An AIM is actually an approximation of the solution of the PDE for sufficiently large time and applicable regardless of the existence of an IM. The smallness of the higher modes in the large time limit has been used to construct an AIM for the 2D NSE and the distance between the AIM and an arbitrary solution has been estimated.

Many PDEs, including NSE and MHD equations, can be written in the form of an abstract evolution equation in an appropriate Hilbert space H. Let u be the solution to the abstract flow equation in H,

$$\frac{\mathrm{d}u}{\mathrm{d}t} + Au + B(u) = f \tag{1}$$

where $f \in H$, A is a linear, self-adjoint, positive operator and B is a nonlinear operator in H. We assume that for all initial values $u_0 \in H$ there exists a unique solution of equation (1) satisfying the initial condition $u(0) = u_0$. Furthermore, we assume that there exists a complete orthonormal system of eigenvectors $\{v_j\}_{j=1}^{\infty}$ of A in H:

$$Av_j = \lambda_j v_j \qquad j \in \mathbb{N}$$
$$0 < \lambda_1 \leqslant \lambda_2, \ldots \qquad \lambda_j \to \infty \qquad \text{as } j \to \infty.$$

Let $p = P_m u$ denote the projection of u onto the finite-dimensional space spanned by the first m eigenvectors of A (lower modes) and $q = Q_m u$ denote the projection of u onto the infinite-dimensional space spanned by the remaining eigenvectors of A (higher modes). Then equation (1) can be written equivalently as a coupled system of equations for p and q,

$$\frac{\mathrm{d}p}{\mathrm{d}t} + Ap + P_m B(p+q) = P_m f \tag{2}$$

$$\frac{\mathrm{d}q}{\mathrm{d}t} + Aq + Q_m B(p+q) = Q_m f. \tag{3}$$

P_m and Q_m are the projectors onto the finite- and infinite-dimensional linear subspaces of H. To solve equation (1) numerically one has to approximate it using a finite system of ODEs.

When applying the linear Galerkin method the higher modes q are neglected in equation (2) leading to an approximate solution u_m in a finite-dimensional phase space $P_m H$,

$$\frac{\mathrm{d}u_m}{\mathrm{d}t} + Au_m + P_m B(u_m) = P_m f. \tag{4}$$

Foias *et al* (1988b) have shown that for 2D NSE a reasonable approximation to equation (3) is given by

$$Aq + Q_m B(p) = Q_m f. \tag{5}$$

This led them to introduce a finite-dimensional manifold by

$$\Phi_{\mathrm{AIM}}(p) := A^{-1}(Qf - Q_m B(p)). \tag{6}$$

The function Φ_{AIM} defines an AIM and represents the small-scale components q in an approximate way as a function of the large-scale components p of the solution. Any solution $u = p + q$ to the 2D NSE satisfies

$$\limsup_{t\to\infty} q(t) - \Phi_{\mathrm{AIM}}(p(t))| \leqslant c_m \tag{7}$$

with constants c_m that, as m tends to infinity, tend to zero much faster than $\limsup_{t\to\infty} |q(t)|$.

In order to determine the number of relevant degrees of freedom which characterize the qualitative behaviour of solutions a finite number of determining modes has been estimated by Foias and Prodi (1967) for 2D NSE.

According to a definition introduced by Foias and Prodi (1967), m is said to be the number of determining modes if for any two solutions u_1, u_2 to equation (1)

$$\lim_{t\to\infty} |p_1 - p_2| = 0 \qquad \text{implies } \lim_{t\to\infty} |q_1 - q_2| = 0$$

where $p_i = P_m u_i$, $q_i = Q_m u_i$ and $u_i = p_i + q_i$ $(i = 1, 2)$. This criterion is clearly satisfied for solutions on an IM, since in this case

$$\lim_{t\to\infty} |q_1 - q_2| = \lim_{t\to\infty} |\Phi_{\mathrm{IM}}(p_1) - \Phi_{\mathrm{IM}}(p_2)| \leqslant l \lim_{t\to\infty} |p_1 - p_2|$$

with l denoting a Lipschitz constant of Φ_{IM}.

The Fourier coefficients of these determining modes, which are active modes for nonlinear Galerkin methods, are calculated as solutions of a finite-dimensional system of ODEs, while the influence of the remaining modes is considered in the form of a slaving function.

This paper is organized as follows. In section 2 we introduce the MHD equations, while in section 3 we estimate the number of determining modes and describe the implementation of Galerkin methods. In section 4 we compare numerically the number of necessary equations, as well as the computational efficiency for both linear and nonlinear Galerkin methods.

2. MHD equations

A central problem in the theory of electrically conducting fluids is the explanation of the origin of cosmical magnetic fields, such as those of the Earth and the Sun (Roberts and Soward 1992). The majority of studies in this field have been kinematic. Kinematic dynamo theory studies the conditions under which a prescribed velocity field can amplify or at least prevent from decaying, some seed magnetic field, completely disregarding the equations governing the motion of the fluid. The hitherto most successful branch of kinematic dynamo theory is the theory of turbulent dynamo (Moffatt 1978, Krause and Rädler 1980), which

has supplied evidence that the presence of kinetic and magnetic helicity at small scales is the motor of growth of the large-scale magnetic field. By imposing a forcing which produces a strong kinetic helicity we have studied the complete system of the incompressible MHD equations.

The equations which we are interested in are given in a domain $\Omega \subset \mathbb{R}^3$, occupied by a nonrelativistic, incompressible, viscous fluid with finite electrical conductivity. The unknown functions are fluid velocity $\boldsymbol{u}$, magnetic field $\boldsymbol{B}$ and thermal pressure p. The density is supposed to be homogeneous and for simplicity set equal to unity. Then the equations can be written as (Roberts 1967, Sermange and Temam 1983)

$$\frac{\partial \boldsymbol{u}}{\partial t} + (\boldsymbol{u}\cdot\nabla)\boldsymbol{u} - \nu\cdot\Delta\boldsymbol{u} + \operatorname{grad} p + \tfrac{1}{2}\operatorname{grad}\boldsymbol{B}^2 - (\boldsymbol{B}\cdot\nabla)\boldsymbol{B} = \boldsymbol{f} \qquad \text{in } \Omega \tag{8}$$

$$\frac{\partial \boldsymbol{B}}{\partial t} + (\boldsymbol{u}\cdot\nabla)\boldsymbol{B} - (\boldsymbol{B}\cdot\nabla)\boldsymbol{u} - \eta\cdot\Delta\boldsymbol{B} = 0 \qquad \text{in } \Omega \tag{9}$$

$$\operatorname{div}\boldsymbol{u} = 0 \qquad \text{in } \Omega \qquad \operatorname{div}\boldsymbol{B} = 0 \qquad \text{in } \Omega \tag{10}$$

where ν and η denote kinetic viscosity and magnetic diffusivity (both assumed constant), and $\boldsymbol{f}$ is an externally applied volume force. Equations (8)–(10) are completed by initial and boundary conditions upon $\boldsymbol{u}$ and $\boldsymbol{B}$. We restrict ourselves to the case of periodic boundary conditions,

$$\begin{gathered}\boldsymbol{u}(\boldsymbol{x}+2\pi e_i,t) = \boldsymbol{u}(\boldsymbol{x},t) \qquad \boldsymbol{B}(\boldsymbol{x}+2\pi e_i,t) = \boldsymbol{B}(\boldsymbol{x},t) \qquad \boldsymbol{x}\in[0,2\pi]^3 \\ \frac{\partial \boldsymbol{u}_j}{\partial x_k}(x+2\pi e_i,t) = \frac{\partial \boldsymbol{u}_j}{\partial x_k}(\boldsymbol{x},t) \qquad \frac{\partial \boldsymbol{B}_j}{\partial x_k}(\boldsymbol{x}+2\pi e_i,t) = \frac{\partial \boldsymbol{B}_j}{\partial x_k}(\boldsymbol{x},t) \qquad \boldsymbol{x}\in[0,2\pi]^3\end{gathered} \tag{11}$$

where $(e_i)_{i=1}^3$ is an orthonormal basis of $\mathbb{R}^3$, $j,k = 1\ldots 3$.

The mean values of $\boldsymbol{u}$ and $\boldsymbol{B}$, and consequently also of $\boldsymbol{f}$, are assumed to vanish,

$$\int_{[0,2\pi]^3} \boldsymbol{u}\,\mathrm{d}^3\boldsymbol{x} = 0 \qquad \int_{[0,2\pi]^3} \boldsymbol{B}\,\mathrm{d}^3\boldsymbol{x} = 0 \qquad \int_{[0,2\pi]^3} \boldsymbol{f}\,\mathrm{d}^3\boldsymbol{x} = 0. \tag{12}$$

The periodicity assumption implies that

$$\exp(\mathrm{i}\boldsymbol{k}\cdot\boldsymbol{x}) \qquad \boldsymbol{k}\in\mathbb{Z}^3$$

is a complete orthonormal system of eigenvectors of the Laplacian with eigenvalues

$$\lambda_{\boldsymbol{k}} = \boldsymbol{k}^2 \qquad \boldsymbol{k}\in\mathbb{Z}^3$$

and that Fourier representations of $\boldsymbol{u}$, $\boldsymbol{B}$, p, and $\boldsymbol{f}$,

$$\boldsymbol{u}(\boldsymbol{x},t) = \sum_{\boldsymbol{k}\in\mathbb{Z}^3,\boldsymbol{k}\neq 0} \boldsymbol{u}_{\boldsymbol{k}}(t)\exp(\mathrm{i}\boldsymbol{k}\cdot\boldsymbol{x}) \qquad \boldsymbol{B}(\boldsymbol{x},t) = \sum_{\boldsymbol{k}\in\mathbb{Z}^3,\boldsymbol{k}\neq 0} \boldsymbol{B}_{\boldsymbol{k}}(t)\exp(\mathrm{i}\boldsymbol{k}\cdot\boldsymbol{x}) \tag{13}$$

$$p(\boldsymbol{x},t) = \sum_{\boldsymbol{k}\in\mathbb{Z}^3,\boldsymbol{k}\neq 0} p_{\boldsymbol{k}}(t)\exp(\mathrm{i}\boldsymbol{k}\cdot\boldsymbol{x}) \qquad \boldsymbol{f}(\boldsymbol{x}) = \sum_{\boldsymbol{k}\in\mathbb{Z}^3,\boldsymbol{k}\neq 0} \boldsymbol{f}_{\boldsymbol{k}}\exp(\mathrm{i}\boldsymbol{k}\cdot\boldsymbol{x}) \tag{14}$$

can be differentiated term by term with respect to the spatial coordinates. In Fourier space equation (10) takes the form

$$\boldsymbol{u}_{\boldsymbol{k}}\cdot\boldsymbol{k} = 0 \qquad \boldsymbol{B}_{\boldsymbol{k}}\cdot\boldsymbol{k} = 0 \tag{15}$$

and is automatically satisfied if we write

$$\boldsymbol{u}_{\boldsymbol{k}} = u_{\boldsymbol{k}}^{(1)}\boldsymbol{e}_{\boldsymbol{k}}^{(1)} + u_{\boldsymbol{k}}^{(2)}\boldsymbol{e}_{\boldsymbol{k}}^{(2)} \qquad \boldsymbol{B}_{\boldsymbol{k}} = B_{\boldsymbol{k}}^{(1)}\boldsymbol{e}_{\boldsymbol{k}}^{(1)} + B_{\boldsymbol{k}}^{(2)}\boldsymbol{e}_{\boldsymbol{k}}^{(2)} \qquad \text{for } \boldsymbol{k}\neq 0 \tag{16}$$

with real 'polarization' unit vectors $\boldsymbol{e}_{\boldsymbol{k}}^{(1)}, \boldsymbol{e}_{\boldsymbol{k}}^{(2)}$ perpendicular to $\boldsymbol{k}$,

$$\boldsymbol{e}_{\boldsymbol{k}}^{(i)}\cdot\boldsymbol{k} = 0 \qquad \boldsymbol{e}_{\boldsymbol{k}}^{(1)}\cdot\boldsymbol{e}_{\boldsymbol{k}}^{(2)} = 0 \qquad \boldsymbol{e}_{\boldsymbol{k}}^{(i)}\cdot\boldsymbol{e}_{\boldsymbol{k}}^{(i)} = 1 \qquad \boldsymbol{e}_{-\boldsymbol{k}}^{(i)} = \boldsymbol{e}_{\boldsymbol{k}}^{(i)} \qquad i = 1,2. \tag{17}$$

The last condition in equation (17) ensures that

$$\boldsymbol{u}_{-\boldsymbol{k}} = \boldsymbol{u}_{\boldsymbol{k}}^* \qquad \boldsymbol{B}_{-\boldsymbol{k}} = \boldsymbol{B}_{\boldsymbol{k}}^* \tag{18}$$

for real $\boldsymbol{u}(\boldsymbol{x})$ and $\boldsymbol{B}(\boldsymbol{x})$ (an asterisk indicates the complex conjugate). By using these representations for $\boldsymbol{u}_{\boldsymbol{k}}$ and $\boldsymbol{B}_{\boldsymbol{k}}$ we discard both the thermal, grad p, and magnetic, grad $\boldsymbol{B}^2/2$, pressure terms in equation (8) and arrive at the following infinite-dimensional system of ODEs:

$$\frac{\mathrm{d}u_{\boldsymbol{k}}^{(j)}}{\mathrm{d}t} = -\nu\boldsymbol{k}^2 u_{\boldsymbol{k}}^{(j)} - \mathrm{i}\sum_{\substack{\boldsymbol{p}\in\mathbb{Z}^3\\ \boldsymbol{p}\neq 0,\boldsymbol{k}}}\sum_{\alpha,\beta=1}^{2}(\boldsymbol{e}_{\boldsymbol{p}}^{(\alpha)}\cdot\boldsymbol{e}_{\boldsymbol{k}}^{(j)})(\boldsymbol{e}_{\boldsymbol{k}}^{(\beta)}\cdot\boldsymbol{k})[u_{\boldsymbol{p}}^{(\alpha)}u_{\boldsymbol{k}-\boldsymbol{p}}^{(\beta)} - B_{\boldsymbol{p}}^{(\alpha)}B_{\boldsymbol{k}-\boldsymbol{p}}^{(\beta)}] + f_{\boldsymbol{k}}^{(j)} \tag{19}$$

$$\frac{\mathrm{d}B_l^{(j)}}{\mathrm{d}t} = -\eta\boldsymbol{k}^2 B_{\boldsymbol{k}}^{(j)} - \mathrm{i}\sum_{\substack{\boldsymbol{p}\in\mathbb{Z}^3\\ \boldsymbol{p}\neq 0,\boldsymbol{k}}}\sum_{\alpha,\beta=1}^{2}(\boldsymbol{e}_{\boldsymbol{p}}^{(\alpha)}\cdot\boldsymbol{e}_{\boldsymbol{k}}^{(j)})(\boldsymbol{e}_{\boldsymbol{k}-\boldsymbol{p}}^{(\beta)}\cdot\boldsymbol{k})[B_{\boldsymbol{p}}^{\alpha)}u_{\boldsymbol{k}-\boldsymbol{p}}^{(\alpha)} - u_{\boldsymbol{k}-\boldsymbol{p}}^{(\beta)}u_{\boldsymbol{p}}^{(\alpha)}B_{\boldsymbol{k}-\boldsymbol{p}}^{(\beta)}]. \tag{20}$$

$f_{\boldsymbol{k}}^{j}$ on the right of equation (19) is defined by

$$f_{\boldsymbol{k}}^{j} = \boldsymbol{f}_{\boldsymbol{k}}\cdot\boldsymbol{e}_{k}^{(j)} \qquad j = 1, 2. \tag{21}$$

Owing to condition (18) we can restrict ourselves to $\boldsymbol{k}$ vectors in a subset $\mathbb{K}$ of $\mathbb{Z}^3$, defined by

$$\mathbb{K} := \{(k_1, k_2, k_3) \in \mathbb{Z}^3 : k_3 > 0\} \cup \{(k_1, k_2, 0) \in \mathbb{Z}^3 : k_1 > 0\} \cup \{(0, k_2, 0) \in \mathbb{Z}^3 : k_2 > 0\}.$$

It has been useful for our calculations to segment $\mathbb{K}$ into successive shells of $\boldsymbol{k}$ vectors

$$\mathbb{K}_i := \{\boldsymbol{k} \in \mathbb{K} : \boldsymbol{k}^2 = i\} \qquad i = 1, 2\ldots$$

$$\mathbb{K} = \bigcup_{i=1}^{\infty}\mathbb{K}_i;\ \mathbb{K}_i \cap \mathbb{K}_j = \emptyset \qquad i, j \in \mathbb{N}, i \neq j.$$

An overview of the segmentation is given in the appendix.

We have used the forcing

$$\boldsymbol{f} = \nu\boldsymbol{u}_{\mathrm{ABC}} \tag{22}$$

where $\boldsymbol{u}_{\mathrm{ABC}}$ is an ABC flow (named after Arnold, Beltami and Childress),

$$\boldsymbol{u}_{\mathrm{ABC}}(x, y, z) = (A\sin k_0 z + C\cos k_0 y,\ B\sin k_0 x + A\cos k_0 z,\ C\sin k_0 y + B\cos k_0 x)$$

where A, B, C are constants and k_0 is the wavenumber of the forced mode (for a rather comprehensive account of the ABC flows see Dombre *et al* (1986)). The ABC flows are Beltrami fields, namely, $\mathrm{curl}\,\boldsymbol{u}_{\mathrm{ABC}} \times \boldsymbol{u}_{\mathrm{ABC}} = \boldsymbol{0}$; thus they are strongly helical. In general (if $ABC \neq 0$), there are domains in the flow where the streamlines are chaotic. It is for these two reasons that the ABC flows have received much interest in the context of kinematic dynamo theory (cf Galloway and Frisch 1986).

The ABC flows are steady solutions of the incompressible Euler equation. They are also steady solutions of the incompressible NSE if an external forcing as given by equation (22) is applied to compensate for viscous losses. The bifurcation properties of the NSE with ABC forcing have been investigated by Podvigina and Pouquet (1994), while the MHD equations with this kind of forcing have been investigated by Galanti *et al* (1992), Feudel *et al* (1995a, 1996) and Seehafer *et al* (1996).

Throughout our calculations we have used a forcing according to equation (22) with

$$k_0 = 1 \qquad A = B = C = f$$

and have, following Galanti *et al* (1992), defined the kinetic and magnetic Reynolds numbers R and R_m by

$$R = \frac{f}{\nu} \qquad Rm = \frac{f}{\eta}.$$

While restricting ourselves to the case $\nu = \eta$ (magnetic Prandtl number equal to unity), R has been our bifurcation parameter.

3. Determining modes and implementation of Galerkin methods

It has been shown by several authors that by using AIMs the distance between the exact solution to equation (1) and the approximate solution can be reduced compared with a simple Fourier truncation, see for example, Titi (1990) and Marion and Temam (1989) for 2D NSE. However, there are no estimates in general which tell how the functions $p = P_m u$ and $p + \Phi_{\mathrm{AIM}}(p)$ are related to the exact solution u or how large m must be in equation (4) to obtain at least a qualitatively correct approximation.

To obtain a suggestion of which modes have to be used as active modes and which have to be used as slaved modes for nonlinear Galerkin methods we estimate the number of determining modes. First we estimate the number of determining modes in the sense defined by Foias and Prodi and second we give some estimates based on a generalized definition of determining modes. It is important to mention that these estimates do not give an absolute number of active modes, but justify a numerical search for these determining modes. Thus, the final number must be determined for every different problem numerically.

Following Constantin *et al* (1985) we give a definition of determining modes. Let $\boldsymbol{u}_i, \boldsymbol{B}_i$ $(i = 1, 2)$ be two solutions to equations (8)–(11) starting from different initial values with Fourier representation (13) and Fourier coefficients $\boldsymbol{u}_{\boldsymbol{k}}^i$ and $\boldsymbol{B}_{\boldsymbol{k}}^i$.

Definition 3.1. $m_0 \in \mathbb{N}$ is said to be the number of determining modes of equations (8)–(11) if

$$\begin{aligned} &\text{from } \lim_{t\to\infty} |\boldsymbol{u}_{\boldsymbol{k}}^1(t) - \boldsymbol{u}_{\boldsymbol{k}}^2(t)| = 0 \qquad \lim_{t\to\infty} |\boldsymbol{B}_{\boldsymbol{k}}^1(t) - \boldsymbol{B}_{\boldsymbol{k}}^2(t)| = 0 \qquad \boldsymbol{k}^2 \leqslant m_0 \\ &\text{follow } \lim_{t\to\infty} |\boldsymbol{u}_{\boldsymbol{k}}^1(t) - \boldsymbol{u}_{\boldsymbol{k}}^2(t)| = 0 \qquad \lim_{t\to\infty} |\boldsymbol{B}_{\boldsymbol{k}}^1(t) - \boldsymbol{B}_{\boldsymbol{k}}^2(t)| = 0 \qquad \boldsymbol{k} \in \mathbb{Z}^3 \end{aligned} \tag{23}$$

for any two solutions $\boldsymbol{u}_1, \boldsymbol{B}_1$ and $\boldsymbol{u}_2, \boldsymbol{B}_2$ to equations (8)–(11).

While estimating the number of determining modes a necessary and sufficient condition for m_0 to be the number of determining modes is given via a lower bound for the eigenvalues of the Laplacian, $\lambda_k = \boldsymbol{k}^2$ $\boldsymbol{k} \in \mathbb{Z}^3$, which is explicitly derived in Schmidtmann (1996). Using this condition the eigenvectors are taken into account only by their eigenvalues which implies that one cannot distinguish between eigenvectors corresponding to the same eigenvalue.

In order to obtain a more accurate estimate of the number of determining modes in the following we shall not give a condition for the eigenvalues but characterize the determining modes by the enstrophy of the Fourier coefficients, which is the energy of the Fourier coefficients multiplied by the corresponding eigenvalue (see section 4.3). In contrast to definition 3.1, where the determining modes are chosen according to the size of their eigenvalues, which may be the same for a large number of eigenvectors, we are now able to check for every single eigenvector the quality to be determining or not. With this characterization it is possible to distinguish between eigenvectors belonging to one and the same eigenvalue and to give a more precise subdivision of the eigenvectors into determining and slaved modes.

A more precise characterization of determining modes has been used to define generalized nonlinear Galerkin methods. This is explained in the following.

For linear Galerkin methods LGM(m) we restrict equations (19)–(20) to a finite set of $\boldsymbol{k}$ vectors such that $\boldsymbol{k}, \boldsymbol{p}$ and $\boldsymbol{k}-\boldsymbol{p}$ belong to shells $1 \ldots m$. To implement nonlinear Galerkin methods NLGM(m, n) we represent coefficients of wavevectors in shells $m+1 \ldots n$, $1 < m < n$ in terms of the coefficients of wavevectors in shells $1 \ldots m$ according to the definition of Φ_{AIM} (see equation (6)) by

$$u_{\boldsymbol{k}}^{(j)} := \frac{-\mathrm{i}}{\nu \boldsymbol{k}^2} \sum_{\substack{\boldsymbol{p} \in \cup_{i=1}^{m} \mathbb{K}_i \\ \boldsymbol{p} \neq 0, \boldsymbol{k}}} \sum_{\alpha,\beta=1}^{2} (\boldsymbol{e}_{\boldsymbol{p}}^{(\alpha)} \cdot \boldsymbol{e}_{\boldsymbol{k}}^{(j)})(\boldsymbol{e}_{\boldsymbol{k}-\boldsymbol{p}}^{(\beta)} \cdot \boldsymbol{k})[u_{\boldsymbol{p}}^{(\alpha)} u_{\boldsymbol{k}-\boldsymbol{p}}^{(\beta)} - B_{\boldsymbol{p}}^{(\alpha)} B_{\boldsymbol{k}-\boldsymbol{p}}^{(\beta)}] + \frac{f_{\boldsymbol{k}}^{(j)}}{\nu \boldsymbol{k}^2} \tag{24}$$

and

$$B_{\boldsymbol{k}}^{(j)} := \frac{-\mathrm{i}}{\eta \boldsymbol{k}^2} \sum_{\substack{\boldsymbol{p} \in \cup_{i=1}^{m} \mathbb{K}_i \\ \boldsymbol{p} \neq 0, \boldsymbol{k}}} \sum_{\alpha,\beta=1}^{2} (\boldsymbol{e}_{\boldsymbol{p}}^{(\alpha)} \cdot \boldsymbol{e}_{\boldsymbol{k}}^{(j)})(\boldsymbol{e}_{\boldsymbol{k}-\boldsymbol{p}}^{(\beta)} \cdot \boldsymbol{k})[B_{\boldsymbol{p}}^{(\alpha)} u_{\boldsymbol{k}-\boldsymbol{p}}^{(\beta)} - u_{\boldsymbol{p}}^{(\alpha)} B_{\boldsymbol{k}-\boldsymbol{p}}^{(\beta)}]. \tag{25}$$

If we take $\boldsymbol{p}$ and $\boldsymbol{k}$ such that $\boldsymbol{p}^2 \leqslant m$ and $(k-p)^2 \leqslant m$ we find

$$\boldsymbol{k}^2 = ((\boldsymbol{k}-\boldsymbol{p})+\boldsymbol{p})^2 = (\boldsymbol{k}-\boldsymbol{p})^2 + 2(\boldsymbol{k}-\boldsymbol{p}) \cdot \boldsymbol{p} + \boldsymbol{p}^2 \leqslant 4m$$

and therefore we always choose $n \leqslant 4m$. Solutions to LGM(m) and NLGM(m, n) are denoted by $\boldsymbol{u}_m, \boldsymbol{B}_m$, while the correction terms for nonlinear Galerkin methods are $\boldsymbol{z}_m$ for the velocity and $\boldsymbol{Z}_m$ for the magnetic field ($(\boldsymbol{z}_m, \boldsymbol{Z}_m) = \Phi_{\mathrm{AIM}}(\boldsymbol{u}_m, \boldsymbol{B}_m)$).

The active modes, in the sense of the generalized definition of finite sets of determining modes, are not necessarily the first modes of a Fourier series and we try to characterize them by their enstrophy. Therefore in the following the nonlinear Galerkin methods are modified in such a way that lower modes can also be slaved modes and higher modes could be active modes we measure the entropy of the coefficients of the Fourier modes. The modes whose time-averaged enstrophy is small are slaved in terms of the modes containing most of the enstrophy.

We assume that the solutions $\boldsymbol{u}_m$ and $\boldsymbol{B}_m$ to LGM(m) are known for sufficiently large m. We define for the coefficients of these solutions

$$\Gamma(\boldsymbol{u}_{\boldsymbol{k}}) := \limsup_{t \to \infty} \frac{1}{t} \int \boldsymbol{u}_{\boldsymbol{k}}^2(\tau)\, \mathrm{d}\tau \qquad \boldsymbol{k} \in \bigcup_{i=1}^{m} \mathbb{K}_i$$

$$\Gamma(\boldsymbol{B}_{\boldsymbol{k}}) := \limsup_{t \to \infty} \frac{1}{t} \int_0^t \boldsymbol{B}_{\boldsymbol{k}}^2(\tau)\, \mathrm{d}\tau \qquad \boldsymbol{k} \in \bigcup_{i-1}^{m} \mathbb{K}_i.$$

Furthermore we look for vectors $\boldsymbol{k}_{\boldsymbol{u}}^*$ and $\boldsymbol{k}_{\boldsymbol{B}}^*$ such that

$$\Gamma(\boldsymbol{u}_{\boldsymbol{k}_{\boldsymbol{u}}^*}) \cdot \boldsymbol{k}_{\boldsymbol{u}}^{*2} \geqslant \Gamma(\boldsymbol{u}_{\boldsymbol{k}}) \cdot \boldsymbol{k}^2 \qquad \Gamma(\boldsymbol{B}_{\boldsymbol{k}_{\boldsymbol{B}}^*}) \cdot \boldsymbol{k}_{\boldsymbol{B}}^{*2} \geqslant \Gamma(\boldsymbol{B}_{\boldsymbol{k}}) \cdot \boldsymbol{k}^2 \qquad \boldsymbol{k} \in \bigcup_{i=1}^{m} \mathbb{K}_i.$$

By means of these quantities we define the sets of relevant modes for velocity and magnetic field

$$\mathcal{N}_{\boldsymbol{u}} := \left(\boldsymbol{k} \in \bigcup_{i=1}^{m} \mathbb{K}_i : \Gamma(\boldsymbol{u}_{\boldsymbol{k}}) \cdot \boldsymbol{k}^2 \geqslant \varepsilon \cdot \Gamma(\boldsymbol{u}_{\boldsymbol{k}_{\boldsymbol{u}}^*}) \cdot \boldsymbol{k}_{\boldsymbol{u}}^{*2} \right) \qquad 0 \leqslant \varepsilon \leqslant 1$$

and

$$\mathcal{N}_{\boldsymbol{B}} := \left(\boldsymbol{k} \in \bigcup_{i=1}^{m} \mathbb{K}_i : \Gamma(\boldsymbol{B}_{\boldsymbol{k}}) \cdot \boldsymbol{k}^2 \geqslant \varepsilon \cdot \Gamma(\boldsymbol{B}_{\boldsymbol{k}_{\boldsymbol{B}}^*}) \cdot \boldsymbol{k}_{\boldsymbol{B}}^{*2} \right) \qquad 0 \leqslant \varepsilon \leqslant 1.$$

In the case $\varepsilon = 0$ there holds of course

$$\mathcal{N}_{\boldsymbol{u}} = \mathcal{N}_{\boldsymbol{B}} = \bigcup_{i=1}^{m} \mathbb{K}_i .$$

For the sets $\mathcal{N}_{\boldsymbol{u}}$ and $\mathcal{N}_{\boldsymbol{B}}$ of vectors, whose coefficients can be considered as active modes we define generalized nonlinear Galerkin methods NLGM(ε, m, n), $1 \leqslant m \leqslant n$, $0 \leqslant \varepsilon \leqslant 1$ as a finite system of ODEs for the coefficients

$$\boldsymbol{u}_{\boldsymbol{k}} : \boldsymbol{k} \in \bigcup_{i=1}^{m} \mathbb{K}_i \cap \mathcal{N}_{\boldsymbol{u}} \qquad \text{and} \qquad \boldsymbol{B}_{\boldsymbol{k}} : \boldsymbol{k} \in \bigcup_{i=1}^{m} \mathbb{K}_i \cap \mathcal{N}_{\boldsymbol{B}}$$

(active modes). The coefficients

$$\boldsymbol{u}_{\boldsymbol{k}} : \boldsymbol{k} \in \bigcup_{i=1}^{n} \mathbb{K}_i \setminus \left(\bigcup_{i=1}^{m} \mathbb{K}_i \cap \mathcal{N}_{\boldsymbol{u}} \right)$$

are calculated as a generalization of (24) by

$$u_{\boldsymbol{k}}^{(j)} := \frac{f_{\boldsymbol{k}}^{(j)}}{\nu \boldsymbol{k}^2} - \frac{\mathrm{i}}{\nu \cdot \boldsymbol{k}^2} \Bigg(\sum_{\substack{\boldsymbol{k}-\boldsymbol{p} \\ \boldsymbol{p} \in \cup_{i=1}^{m} \mathbb{K}_i \cap \mathcal{N}_{\boldsymbol{u}}}} \sum_{\alpha,\beta=1}^{2} (\boldsymbol{e}_{\boldsymbol{p}}^{(\alpha)} \cdot \boldsymbol{e}_{\boldsymbol{k}}^{(j)})(\boldsymbol{e}_{\boldsymbol{k}-\boldsymbol{p}}^{(\beta)} \cdot \boldsymbol{k}) u_{\boldsymbol{p}}^{(\alpha)} u_{\boldsymbol{k}-\boldsymbol{p}}^{(\beta)} \Bigg)$$

$$+ \frac{\mathrm{i}}{\nu \cdot \boldsymbol{k}^2} \Bigg(\sum_{\substack{\boldsymbol{k}-\boldsymbol{p} \\ \boldsymbol{p} \in \cup_{i=1}^{m} \mathbb{K}_i \cap \mathcal{N}_{\boldsymbol{B}}}} \sum_{\alpha,\beta=1}^{2} (\boldsymbol{e}_{\boldsymbol{p}}^{(\alpha)} \cdot \boldsymbol{e}_{\boldsymbol{k}}^{(j)})(\boldsymbol{e}_{\boldsymbol{k}-\boldsymbol{p}}^{(\beta)} \cdot \boldsymbol{k}) B_{\boldsymbol{p}}^{(\alpha)} B_{\boldsymbol{k}-\boldsymbol{p}}^{(\beta)} \Bigg) \tag{26}$$

and the coefficients

$$\boldsymbol{B}_{\boldsymbol{k}} : \boldsymbol{k} \in \bigcup_{i=1}^{n} \mathbb{K}_i \setminus \left(\bigcup_{i=1}^{m} \mathbb{K}_i \cap \mathcal{N}_{\boldsymbol{B}} \right)$$

are calculated as a generalization of (25) by

$$B_{\boldsymbol{k}}^{(j)} := \frac{-\mathrm{i}}{\eta \cdot \boldsymbol{k}^2} \Bigg(\sum_{\substack{\boldsymbol{k}-\boldsymbol{p} \\ \boldsymbol{p} \in \cup_{i=1}^{m} \mathbb{K}_i \cap \mathcal{N}_{\boldsymbol{B}}}} \sum_{\alpha,\beta=1}^{2} (\boldsymbol{e}_{\boldsymbol{p}}^{(\alpha)} \cdot \boldsymbol{e}_{\boldsymbol{k}}^{(j)})(\boldsymbol{e}_{\boldsymbol{k}-\boldsymbol{p}}^{(\beta)} \cdot \boldsymbol{k}) [B_{\boldsymbol{p}}^{(\alpha)} u_{\boldsymbol{k}-\boldsymbol{p}}^{(\beta)} - u_{\boldsymbol{p}}^{(\alpha)} B_{\boldsymbol{k}-\boldsymbol{p}}^{(\beta)}] \Bigg). \tag{27}$$

4. Numerical results

For the integration of the equations we used a Runge Kutta method of sixth order where the step size was controlled by a method used by Hairer *et al* (1983).

4.1. Stationary solutions

For sufficiently weak forcing, which is equivalent to a small Reynolds number R, the ABC flow with no magnetic field is the only attracting state. Varying R, we have calculated the eigenvalues of the Jacobian in order to detect bifurcation points. For an increased value of R the primary ABC flow loses stability in a Hopf bifurcation, leading to a periodic solution with a non-vanishing magnetic field.

The influence of the number of active and slaved modes for linear and nonlinear Galerkin methods LGM(m) and NLGM(m, n) onto the critical value of R for the Hopf bifurcation has been investigated by Schmidtmann *et al* (1997). The number of active modes has been reduced by 60% with NLGM(m, n) compared with LGM(m) to compute the critical Reynolds number for the magnetic instability in the corresponding kinematic

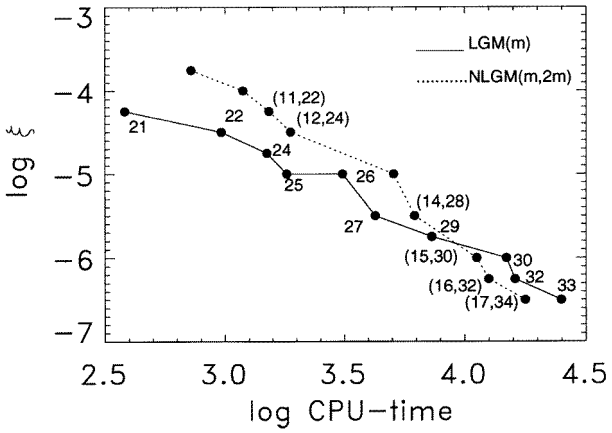

Figure 1. CPU time needed to approximate $\boldsymbol{u}_{37}, \boldsymbol{B}_{37}$ with accuracy ξ for linear Galerkin methods LGM(m) and nonlinear Galerkin methods NLGM($m, 2m$) ($R = 10$).

dynamo problem, for which a value of $R_c = 8.9$ has been found (cf Galloway and Frisch (1986)).

4.2. Accuracy and computational efficiency of nonlinear Galerkin methods

Next we have studied, for a periodic orbit, the influence of the degree of truncation on the quality of the approximation, both for the LGM and the NLGM. We have fixed the Reynolds number at $R = 10$, where a periodic attractor exists if $m \geqslant 21$, and have varied the number of shells taken into account. Another question which we are interested in is whether solutions with the same accuracy as those of LGM($\tilde{m}$) can be obtained by lower computational costs (CPU time) by means of NLGM(m, n). In experiments to address this question, the Reynolds number has been fixed at $R = 10$ and the initial points for the approximate solutions $\boldsymbol{u}_m, \boldsymbol{B}_m$ have been given by the projections $P_7\boldsymbol{u}_{37}(0)$ and $P_7\boldsymbol{B}_{37}(0)$; $\boldsymbol{u}_{37}$ and $\boldsymbol{B}_{37}$ we refer in the following as the 'exact' solution. The distance between the exact and the approximate solution at time t we define by

$$\xi_{\mathrm{LGM}(m)}(t) = (\|\boldsymbol{u}_{37}(t) - \boldsymbol{u}_m(t)\|_{L^2}^2 + \|\boldsymbol{B}_{37}(t) - \boldsymbol{B}_m(t)\|_{L^2}^2)$$

for linear Galerkin methods and

$$\xi_{\mathrm{NLGM}(m,2m)}(t) = (\|\boldsymbol{u}_{37}(t) - (\boldsymbol{u}_m(t) + \boldsymbol{z}_m(t))\|_{L^2}^2 + \|\boldsymbol{B}_{37}(t) - (\boldsymbol{B}_m(t) + \boldsymbol{Z}_m(t))\|_{L^2}^2)$$

for nonlinear Galerkin methods. $\xi_{\mathrm{LGM}(m)}$ and $\xi_{\mathrm{NLGM}(m,2m)}$, respectively, measure the accuracy of the different approximations.

We integrate up to a time $t = t_1$ for LGM(m) and $t = t_2$ for NLGM($m, 2m$), where the quantities $\xi_{\mathrm{LGM}(m)}(t)$ and $\xi_{\mathrm{NLGM}(m,2m)}(t)$ satisfy the inequality

$$\xi_{\mathrm{LGM}(m)}(t_1), \xi_{\mathrm{NLGM}(m,2m)}(t_2) \leqslant \xi \qquad \text{for } \xi = 10^{-6.5+i0.25},\ i = 0 \ldots 9. \quad (28)$$

In figure 1 these accuracies ξ are plotted versus the CPU time needed to integrate up to $t = t_1$ and $t = t_2$, respectively. For larger $m, m > 15$, the use of the nonlinear Galerkin methods allows us to reduce the CPU time by approximately 30% compared with the linear methods.

These plots indicate a better convergence for the nonlinear Galerkin method, which confirms the expectation that the solutions obtained by NLGM(m, n), $n > m$, are more

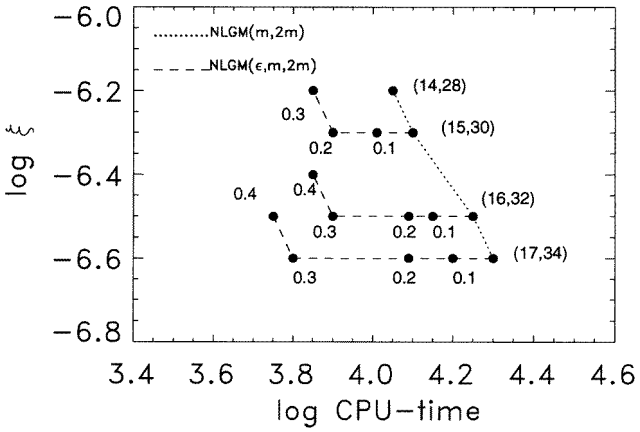

Figure 2. CPU time needed to approximate $\boldsymbol{u}_{34}, \boldsymbol{B}_{34}$ with an accuracy ξ for nonlinear Galerkin method NLGM$(\varepsilon, m, 2m)$ $(R = 10)$.

accurate than those obtained by LGM(m). However, on the other hand the nonlinear Galerkin method NLGM(m, n) cannot be better than the linear method LGM(n) for $n > m$ and loosely speaking, the accuracy of the nonlinear Galerkin method NLGM(m, n) should correspond to that of some LGM$(\tilde{m})$ with $m < \tilde{m} < n$.

Furthermore we have compared the efficiency of the nonlinear Galerkin methods NLGM$(m, 2m)$ and NLGM$(\varepsilon, m, 2m)$ for $14 \leqslant m \leqslant 17$, $0 \leqslant \varepsilon \leqslant 0.4$. In figure 2 the CPU time is plotted which is necessary to approximate the 'exact solution' within a given accuracy

$$\xi = 10^{-6.6+i0.1} \qquad i = 0, \ldots, 3.$$

By using NLGM$(\varepsilon, m, 2m)$ we are able to reduce the CPU time more significantly than by using NLGM$(m, 2m)$. For NLGM$(0.3, 17, 34)$ we can reduce the CPU time compared with NLGM$(17, 34)$ by approximately 70% and compared with LGM(m) by about 75%.

4.3. Kaplan–Yorke dimension for the chaotic regime

Since in the case of chaotic solutions sensitivity to initial conditions would lead to bad accuracy, another criterion, different from that in the case of periodic solutions, has to be applied in order to measure the quality of the approximation of a reference solution. To estimate the number of modes needed to describe the behaviour of the exact solutions in the chaotic regime qualitatively correctly, we have calculated the energy of the flow,

$$\tfrac{1}{2}\|\boldsymbol{u}\|_{L^2}^2 + \tfrac{1}{2}\|\boldsymbol{B}\|_{L^2}^2 = \tfrac{1}{2}(2\pi)^3 \sum_{\boldsymbol{k}\in\mathbb{Z}^3} |\boldsymbol{u}_{\boldsymbol{k}}|^2 + |\boldsymbol{B}_{\boldsymbol{k}}|^2$$

as well as its enstrophy,

$$\|\operatorname{curl}\boldsymbol{u}\|_{L^2}^2 + \|\operatorname{curl}\boldsymbol{B}\|_{L^2}^2$$

which, because of periodic boundary conditions, equals (cf Doering and Gibbon (1995))

$$\|\nabla\boldsymbol{u}\|_{L^2}^2 + \|\nabla\boldsymbol{B}\|_{L^2}^2 = (2\pi)^3 \sum_{\boldsymbol{k}\in\mathbb{Z}^3} \boldsymbol{k}^2(|\boldsymbol{u}_{\boldsymbol{k}}|^2 + |\boldsymbol{B}_{\boldsymbol{k}}|^2).$$

The estimation of the number of determining modes shows that enstrophy decisively influences the number of determining modes.

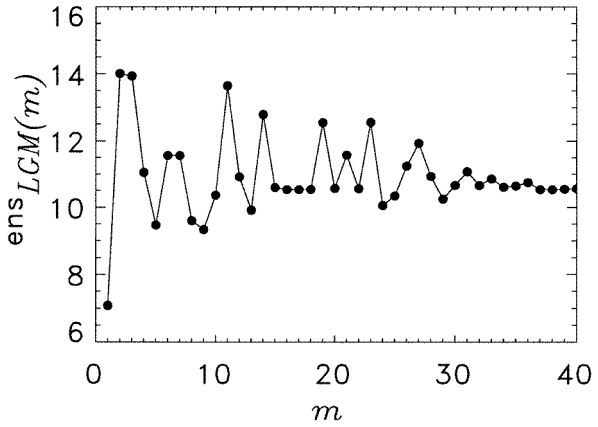

Figure 3. Time average of enstrophy versus the number of shells m containing the active modes for LGM(m) ($R = 20$).

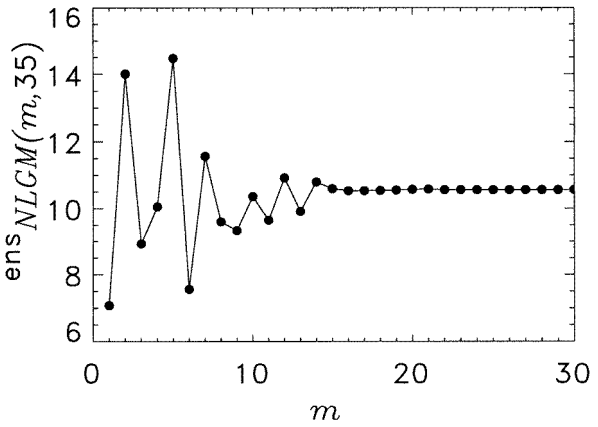

Figure 4. The time average of enstrophy versus the number of shells m containing the active modes for NLGM($m, 35$) ($R = 20$).

The following numerical experiments have been done for a Reynolds number of $R = 20$, for which the solutions are chaotic. Their chaotic character has been verified by calculating the Lyapunov exponents.

For LGM(m) $m^* = 35$ is a saturation point with respect to the calculation of both energy and enstrophy, in the sense that by further increasing m both quantities do not change significantly (see Schmidtmann *et al* (1997)). By applying NLGM($m, 35$) the saturation point is shifted to a smaller number, m, of (active) shells as can be seen in figures 3 and 4.

By using an algorithm of Shimada and Nagashima (1979), for $R = 20$ the largest Lyapunov exponents have been computed and used to calculate the Kaplan–Yorke dimension D_{KY} of the attractor, which provides a good approximation of its Hausdorff dimension (Kaplan and Yorke 1979). If the Lyapunov exponents μ_i are ordered descendingly and j is

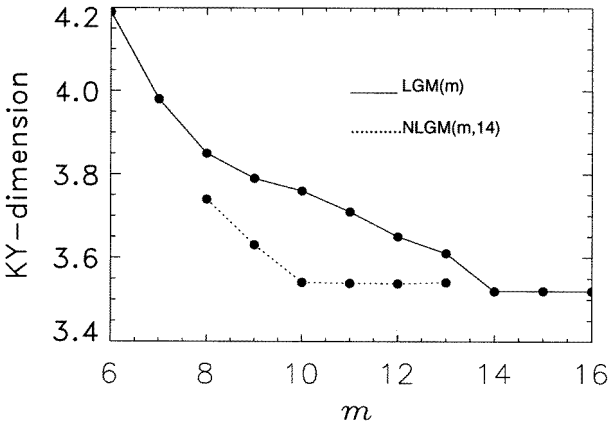

Figure 5. Kaplan–Yorke dimension versus the number of active shells for LGM(m) and NLGM(m, 14) ($R = 20$).

the largest index satisfying

$$\sum_{i=1}^{j} \mu_i \geqslant 0$$

then

$$D_{\mathrm{KY}} = j - \frac{\Sigma_{i=1}^{j} \mu_i}{|\mu_{j+1}|}.$$

Figure 5 gives the Kaplan–Yorke dimensions calculated by means of LGM and NLGM versus the number of active shells. With LGM a saturation is reached at $m = 14$ (while the saturation with respect to energy and enstrophy is reached at $m = 35$). With the nonlinear Galerkin method MLGM(l, 14) the plateau value of the Kaplan–Yorke dimension is reasonably approximated already for $l = 10$. This again suggests that the constructed map ϕ_{AIM} provides an acceptable approximation of the small-scale structures of the flow. By means of NLGM(10,14) we can reduce the CPU time needed to calculate the dimension of the attractor compared with LGM(14) by 25%.

To test the efficiency of linear and nonlinear Galerkin methods in the case of the chaotic solution we have measured the CPU time necessary to calculate the Kaplan–Yorke dimension within a given accuracy for linear and nonlinear Galerkin methods. The initial values for the Galerkin methods LGM(m), NLGM(m, n) and NLGM(ε, m, n) have been chosen on the attractor calculated with these methods. For a given dimension dim we measure the CPU time to reach the dimension

$$\mathrm{dim} = 3.52 + i \cdot 0.5 \qquad i = 0, \ldots, 3.$$

with an accuracy

$$\mathrm{dim} - 0.1 \leqslant D_{\mathrm{KY}} \leqslant \mathrm{dim} + 0.1.$$

In figure 6 it can be seen that with increasing m for LGM(m) the necessary CPU time increases. By means of the NLGM(m, 14) we can reduce the CPU time for NLGM(10, 14) compared with LGM(14) by about 25%. With NLGM(0.2, 10, 14) the CPU time compared with LGM(14) can be reduced by 75%.

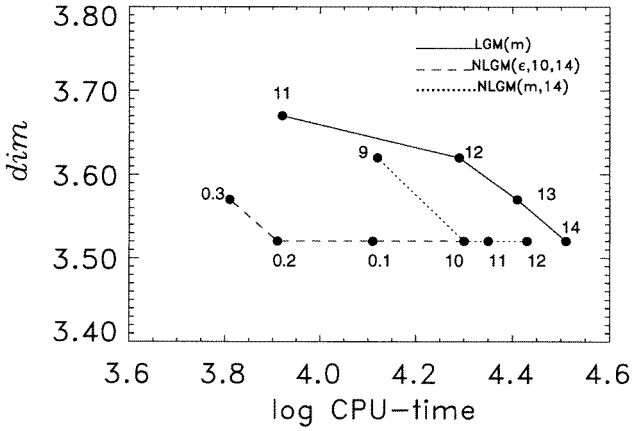

Figure 6. Necessary CPU time needed to calculate a Kaplan–Yorke dimension D_{KY} $\dim - 0.1 \leqslant D_{\mathrm{KY}} \leqslant \dim + 0.1$ with initial value on the attractor of LGM(m), NLGM(m, 14) and NLGM(ε, 10, 14) ($R = 20$).

5. Summary

In this paper we have modified a nonlinear Galerkin method, introduced by Foias *et al* (1988b) for 2D NSE and applied to investigate the long-term behaviour of solutions to three-dimensional (3D) MHD equations. Instead of using the first modes of a Fourier series of the solution as active modes for a nonlinear Galerkin method we have selected the modes containing most of the time-averaged enstrophy as active modes. This was justified by estimating a finite number of determining modes for MHD equations in terms of the time-averaged enstrophy of the Fourier modes. There exists a critical threshold such that the modes whose time-averaged enstrophy is larger than this threshold are determining modes for the solution. With this generalization of the definition of the number of determining modes for the solution. With this generalization of the definition of the number of determining modes introduced by Foias and Prodi (1967) the number of determining modes could be reduced. The absolute number of determining modes, however, can only be estimated numerically. Special bifurcation points, time-averaged values of energy and enstrophy as well as Kaplan–Yorke dimensions have been calculated for both linear and nonlinear schemes in order to compare the efficiency of both methods and to estimate the number of modes necessary to correctly describe the behaviour of the exact solution. While the necessary CPU time to approximate the exact solution could be reduced only slightly for the nonlinear Galerkin methods the modified nonlinear Galerkin methods reduce both the number of necessary equations and the necessary CPU time considerably.

Acknowledgments

This work was supported by the Deutsche Forschungsgemeinschaft (DFG) within its priority research program ‘Ergodentheorie, Analysis und effiziente Simulation dynamischer Systeme’.

Appendix

Table A.1 gives an overview of the partition of $\boldsymbol{k}$ space into successive disjoint shells of $\boldsymbol{k}$ vectors.

Table A.1. Partition of $\boldsymbol{k}$ space.

Number m of shell in $\boldsymbol{k}$ space	Number of $\boldsymbol{k}$ vectors in shell $\mathbb{K}_m$	Number of $\boldsymbol{k}$ vectors in $\cup_{j=1}^{m}\mathbb{K}_j$	Number of ODEs for LGM(m)
1	3	3	24
2	6	9	72
3	4	13	104
4	3	16	128
5	12	28	224
6	12	40	320
7	0	40	320
8	6	46	368
9	15	61	488
10	12	73	584
11	12	85	680
12	4	89	712
13	12	101	808
14	24	125	1000
15	0	125	1000
16	3	128	1024
17	24	152	1216
18	18	170	1360
19	12	182	1456
20	12	194	1552
21	24	218	1744
22	12	230	1840
23	0	230	1840
24	12	242	1936
25	15	257	2056
26	36	293	2344
27	16	309	2472
28	0	309	2472
29	36	345	2760
30	24	369	2952
31	0	369	2952
32	6	375	3000
33	24	399	3192
34	24	423	3384
35	24	447	3576
36	15	462	3696
37	12	474	3792
38	36	510	4080
39	0	510	4080
40	12	522	4176

References

Constantin P, Foias C, Manley O and Temam R 1985 Determining modes and fractal dimension of turbulent flows *J. Fluid Mech.* **150** 427–40

Doering C and Gibbon J 1995 *Applied Analysis of the Navier–Stokes equations* (Cambridge: Cambridge University Press)

Dombre T, Frisch U, Greene J, Hénon M, Mehr A and Soward A 1986 Chaotic streamlines in the ABC flow *J. Fluid Mech.* **167** 353–91

Dubois T, Jaubertau F, Marion F and Temam R 1991 Subgrid modelling and interaction of small and large wavelengths in turbulent flows *Comput. Phys. Commun.* **65** 100–6

Feudel F, Seehafer N, Galanti B and Rüdiger S 1996 Symmetry-breaking bifurcations for the magnetohydrodynamic equations with helical forcing *Phys. Rev.* E **54** 2589–96

Feudel F, Seehafer N and Schmidtmann O 1995a Bifurcation phenomena of the magnetofluid equations *Math. Comput. Simul.* **40** 235–46

——1995b Fluid helicity and dynamo bifurcations *Phys. Lett.* A **202** 73–8

Foias C, Jolly M, Kevrekidis I, Sell G and Titi E 1988a On the computation of inertial manifolds *Phys. Lett.* **131A** 433–6

Foias C, Manley O and Temam R 1988b Modelling of the interaction of small and large eddies in two dimensional turbulent flows *Math. Modelling Numer. Anal.* **22** 93–114

Foias C, Nicolaenko B, Sell G and Temam R 1988c Inertial manifolds for the Kuramoto–Sivashinsky equation and an estimate of their lowest dimension *J. Math. Pures Appl.* **67** 197–226

Foias C and Prodi G 1967 Sur le comportement global des solutions non stationnaires des équations de Navier–Stokes on dimensional 2 *Rend. Sem. Mat. Univ. Padova* **39** 1

Foias C, Sell G and Temam R 1988 Inertial manifolds for nonlinear evolutionary equations *J. Differ. Equ.* **73** 309–53

Foias C, Sell G and Titi E 1989 Exponential tracking and approximation of inertial manifolds for dissipative nonlinear equations *J. Dyn. Differ. Equ.* **1** 199–244

Frisch U, She Z and Thual O 1986 Viscoelastic behaviour of cellular solutions to the Kuramoto–Sivashinsky model *J. Fluid. Mech.* **168** 221–40

Galanti B, Sulem P and Pouquet A 1992 Linear and non-linear dynamos associated with ABC flows *Geophys. Astrophys. Fluid Dyn.* **66** 183–208

Galloway D and Frisch U 1986 Dynamo action in a family of flows with chaotic streamlines *Geophys. Astrophys. Fluid Dyn.* **36** 53–83

Hairer E, Nørsett S and Wanner G 1983 *Solving Ordinary Differential Equations, Part I–Nonstiff Problems* (Berlin: Springer)

Jauberteau F, Rosier C and Temam R 1989/90 The nonlinear Galerkin method in computational fluid mechanics *Appl. Numer. Math.* **6** 361–70

Kaplan J and Yorke J 1979 Chaotic behavior of multidimensional difference equations *Functional Differential Equations and Approximations of Fixed Points (Springer Lecture Notes in Mathematics 730)* ed H O Peitgen and H O Walther (Berlin: Springer) pp 228–37

Krause F and Rädler K 1980 *Mean-field Magnetohydrodynamics and Dynamo Theory* (Berlin: Akademie)

Manneville P 1990 *Dissipative Structures and Weak Turbulence* (London: Academic)

Marion M and Temam R 1989 Nonlinear Galerkin methods *SIAM J. Numer. Anal.* **26** 1139–57

Moffatt H 1978 *Magnetic Field Generation in Electrically Conducting Fluids* (Cambridge: Cambridge University Press)

Podvigina O and Pouquet A 1994 On the non-linear stability of the 1:1:1 ABC flow *Physica* **75D** 471–508

Roberts P 1967 *An Introduction to Magnetohydrodynamics* (London: Longmans Green)

Roberts P and Soward A 1992 Dynamo theory *Ann. Rev. Fluid Mech.* **24** 459–512

Schmidtmann O 1996 Nichtlineare Galerkin-Verfahren für die 3D magnetohydrodynamischen Gleichungen *Dissertation* Universität Potsdam

Schmidtmann O, Feudel F and Seehafer N 1997 Nonlinear Galerkin methods for the 3D magnetohydrodynamic equations *Int. J. Bifurcation Chaos* **7** 1497–507

Seehafer N, Feudel F and Schmidtmann O 1996 Nonlinear dynamo with ABC forcing *Astron. Astrophys.* **36** 693–9

Sermange M and Temam R 1983 Some mathematical questions related to the MHD equations *Comment. Pure Appl. Math.* **36** 635–64

Shimada I and Nagashima T 1979 A numerical approach to ergodic problem of dissipative dynamical systems *Progr. Theor. Phys.* **61** 1605–16

Swinney H and Gollub J 1985 *Hydrodynamic Instabilities and the Transition to Turbulence* (Berlin: Springer)

Temam R 1988 *Infinite Dimensional Dynamical Systems in Mechanics and Physics* (New York: Springer)

——1989 Do inertial manifolds apply to turbulence? *Physica* **37D** 146–52

——1990 Inertial manifolds *Math. Intell.* **12** 68–74

Titi E 1990 On approximate inertial manifolds to the Navier–Stokes equations *J. Math. Anal. Appl.* **149** 540–57